ANALYSIS OF RNA EXPRESSION PROFILES IDENTIFIES DYSREGULATED VESICLE TRAFFICKING PATHWAYS IN CREUTZFELDT-JAKOB DISEASE

Anna Bartoletti-Stella[1], Patrizia Corrado[2], Nicola Mometto[2], Simone Baiardi[2], Pascal F. Durrenberger[3], Thomas Arzberger[4,5], Richard Reynolds[6], Hans Kretzschmar[5,†], Sabina Capellari[1,2,*], Piero Parchi[1,7,*].

[1]IRCCS Institute of Neurological Sciences of Bologna, Bellaria Hospital, 40139, Bologna, Italy

[2]Department of Biomedical and NeuroMotor Sciences, DIBINEM, University of Bologna, 40123 Bologna, Italy

[3]Centre for Inflammation and Tissue Repair, UCL Respiratory, University College London, Rayne Building, London, UK.

[4]Department of Psychiatry and Psychotherapy, Ludwig-Maximilians-University Munich, Germany

[5]Center for Neuropathology and Prion Research, Ludwig-Maximilians-University Munich, Germany

[6]Division of Brain Sciences, Imperial College London, London, UK,

[7]Department of Experimental, Diagnostic and Specialty Medicine, DIMES, University of Bologna, 40138 Bologna, Italy

[†] Deceased.

[*] Corresponding authors: sabina.capellari@unibo.it (telephone number +390514966115); piero.parchi@unibo.it (telephone number +390514966740)

ORCID IDs: Anna Bartoletti-Stella 0000-0001-6442-162X, Sabina Capellari 0000-0003-1631-1439, Piero Parchi 0000-0002-9444-9524

ACKNOWLEDGEMENTS

Supported by EU Grant FP6, BNEII No LSHM-CT-2004-503039, the University of Bologna (Grant RFO) and the Gino Galletti Foundation.

KEYWORDS: human prion, sporadic Creutzfeldt-Jakob disease, genome-wide expression, membrane trafficking, retromer, VPS35.

ABSTRACT

Functional genomics applied to the study of RNA expression profiles identified several abnormal molecular processes in experimental prion disease. However, only a few similar studies have been carried out to date in a naturally occurring human prion disease. To better characterize the transcriptional cascades associated with sporadic Creutzfeldt-Jakob disease (sCJD), the most common human prion disease, we investigated the global gene expression profile in samples from the frontal cortex of 10 patients with sCJD and 10 non-neurological controls by microarray analysis. The comparison identified 333 highly differentially expressed genes (hDEGs) in sCJD. Functional enrichment Gene Ontology analysis revealed that hDEGs were mainly associated with synaptic transmission, including GABA (q-value=0.049) and glutamate (q-value=0.005) signaling, and the immune/inflammatory response. Furthermore, the analysis of cellular components performed on hDEGs showed a compromised regulation of vesicle-mediated transport with mainly up-regulated genes related to the endosome (q-value=0.01), lysosome (q-value=0.04), and extracellular exosome (q-value<0.01). A targeted analysis of the retromer core component VPS35 (Vacuolar protein sorting-associated protein 35) showed a down-regulation of gene expression (p=0.006) and reduced brain protein levels (p=0.002). Taken together these results confirm and expand previous microarray expression profile data in sCJD. Most significantly, they also demonstrate the involvement of the endosomal-lysosomal system. Since the latter is a common pathogenic pathway linking together diseases such as Alzheimer's and Parkinson's, it might be the focus of future studies aimed to identify new therapeutic targets in neurodegenerative diseases.

INTRODUCTION

Prion diseases or transmissible spongiform encephalopathies (TSEs) belong to the growing group of protein misfolding disorders that primarily affect the brain. However, unlike the most prevalent diseases of this group, such as Alzheimer's (AD), Lewy body disorders (LBD), and frontotemporal dementias (FTD), prion disease affects several mammalian species and uniquely includes patients that acquired the disease through contaminated sources [1, 2]. Creutzfeldt-Jakob disease (CJD), the most common human prion disease, mainly occurs as a sporadic form of unknown origin (sCJD). However, it can also be linked to mutations in the prion protein gene (*PRNP*) in about 15% of cases [3, 4], or rarely be acquired by accidental transmission through medical procedures or food contaminated with the bovine spongiform encephalopathy agent [5]. The hallmark of prion disease pathogenesis is the conversion of the cellular prion protein (PrP^{C}) into an abnormal conformer (PrP^{Sc}), which is rich in β-sheet, partially protease-resistant and aggregation-prone. In the disease, the spontaneously formed or acquired PrP^{Sc} provides a template for further pathogenic conversion of PrP^{C}, and then spreads from one cell to another [6].

Understanding the cascade of molecular events leading to progressive neurodegeneration and neuroinflammation after the formation and spread of PrP^{Sc} is crucial for the identification of potential therapeutic targets. In recent years, advances in technologies led to the discovery of multiple genes and signaling pathways involved in prion disease pathogenesis. Studies in prion-infected mice, allowing cross-sectional time course experiments from the pre-symptomatic phase, demonstrated a differential expression in genes involved in several pathways including protein synthesis, inflammation, cellular proliferation, lipid metabolism, synapse function, apoptotic pathways, oxidative and endoplasmic reticulum stress, and endosome/lysosome function [7].

More significantly, gene expression data obtained throughout disease progression and from eight distinct mouse strain-prion strain combinations, in the most complete genome-wide transcriptional study performed to date, identified a core of 333 genes related to prion disease. They belonged to various

cellular processes including demyelination, hematopoiesis and complement activation, lysosome protease activity, and glycosaminoglycan metabolism [8]. Similar results have been demonstrated by studying the RNA expression profile in orally infected ruminant species (cattle, sheep, and elk) [7] and macaques [9].

Unlike numerous studies on the transcriptome of animal models, only a few have been performed to date in the naturally occurring human prion disease [10-12]. Although animal models allow the numbers and replications needed to design large-scale studies and the possibility to study the different stages of the disease [10], they are not necessarily comparable to humans [13]. Furthermore, experimental animals can only model the acquired variant of the disease. Although human brain tissues provide only information on the end stage of the disease, and the low average quality of post-mortem RNA might potentially influence the outcomes [14], human tissues studies remain the gold standard [15].

In this study, we analyzed the global gene expression profile in brain samples from sCJD patients. The results confirm that synaptic and immune system functions are significantly affected in sCJD, but also suggest an altered vesicle trafficking also involving the retromer complex.

MATERIALS AND METHODS

Brain tissue collection

The study was approved by the Local Ethics Committee. Grey matter tissue samples were collected from the frontal cortex (middle frontal gyrus) of 10 sCJD brains (5 each from the two commonest disease subtypes, MM1 and VV2) and 10 controls (CTRL) without any history of neurological or psychiatric illnesses. Sporadic CJD subjects and CTRL were matched for age (sCJD=66.9±8.2; CTRL=65.7±10.7) and sex (Males, sCJD=40%; CTRL=50%). Tissue was obtained post-mortem according to a standard

protocol. Tissue from the right hemisphere was frozen in dry ice and kept at -80° C until use, while the left hemisphere was fixed in 10% formalin and processed by paraffin wax embedding.

Sporadic CJD cases were classified as MM1 or VV2 according to established histopathological criteria [16] and PrP^{Sc} typing [17]. All selected cases had tissue quality classified as "optimal" (i.e. body maintained refrigerated (2-4°C) before autopsy and post-mortem delay <36 hours) and showed only mild to moderate changes (e.g. spongiform change, gliosis and neuronal loss) in the frontal cortex at histopathological examination. The latter was chosen as area of interest because it is pathologically involved in all CJD subtypes (19,10), and usually available for sampling. Control brains lacked significant vascular and inflammatory abnormalities. Regarding neurodegenerative changes, they were assessed according to established neuropathological criteria. [18] sCJD and CTRL brains were matched for amyloid-beta (Aβ) (Aβ phase 0= 5 CTRL and 6 sCJD; Aβ phase I-II, 3 CTRL and 2 sCJD, Aβ Thal phase III, 1 CTRL and 1 sCJD, Aβ phase IV= 1 CTRL and 1 sCJD), TDP43 (all negative) and tau-related (tau Braak stage 0= 4 sCJD and 3 CTRL; tau stage 1= 5 sCJD and 5 CTRL; tau stage II: 1 sCJD and 2 CTRL) pathology. Finally, all sCJD brains and all but one CTRL were alpha-synuclein negatives by immunohistochemistry. As only exception, one of the cases initially acquired as a control lacking significant neuropathological abnormalities was found to have a significant Lewy-body related pathology (Braak stage 4) at a second, late revision.

RNA extraction

Total RNA was extracted from the frontal cortex of snap-frozen brain according to an optimized protocol [20] using the RNeasy tissue lipid kit (Qiagen, Mannheim, Germany), and stored at -80°C until use. RNA concentration and purity were assessed by spectrophotometry (NanoDrop ND100, Thermo Fisher Scientific, Waltham, MA, USA). Total RNA quality was tested through capillary electrophoresis

(Bioanalyzer 2100, Agilent Technologies, Santa Clara, CA, USA) and RNA was considered suitable when the integrity quality number (RIN) scored above eight.

Microarray and bioinformatic analysis

The RNA expression profile was analyzed using the Illumina whole-genome HumanRef8 v2 BeadChip (Illumina, California, USA). Briefly, RNA samples were processed for array analysis using the Illumina TotalPrep^{TM}96 RNA Amplification Kit (Ambion, Inc., Austin, Texas, USA). Double-stranded complementary DNA (cDNA) was synthesized from 0.5 µg of total RNA. Using cDNA as template, complementary RNA was synthesized and labelled with biotin and then applied to the arrays using the whole-genome gene expression direct hybridization assay system (Illumina). The BeadChips were scanned with the Illumina BeadArray Reader. The data were extracted and processed by applying a quantile normalization using the Illumina Beadstudio 3.2 software (Illumina). To validate the microarray experiment, we included in the analysis one technical replicate sample and verified the high correlation between the pair samples (Pearson r^2=0.998). Differentially expressed genes (DEGs) were identified by determining the p-values of the *t*-test adjusted with Benjamin-Hochberg False Discovery Rate correction (q-value), and fold-change (FC) [21] by using Pathway Studio Software (Ariadne Genomics Inc., Madrid, Spain). Genes with a $Log_2(FC) \geq |1|$ and q-value ≤ 0.05 were identified as highly DEGs (hDEGs).

Functional analyses on transcriptome data

To correlate gene expression changes to biological functions, we carried out the following analyses:

1) Gene ontology (GO) and pathways analysis of the DEGs. For hDEGs classification, we used GO and the Kyoto Encyclopedia of Genes and Genomes (KEGG), two of the most common databases currently use for functional gene annotation. GO describes the function of genes or proteins in three broad categories: biological process, molecular function, and cellular component. Each of these

categories is represented as a tree structure, in which the nodes are terms, and the branches define their relationships. In annotation databases, individual genes are linked to terms of this tree. KEGG Pathway databases, instead, present biological processes as a succession of reactions among molecules that lead to a certain product or a functional change in the cell, integrating the effect of a genetic factor in the biological network [22]. The Protein ANalysis THrough Evolutionary Relationships (PANTHER) analysis tool was used to categorize DEGs by GO Biological Process and GO Cellular Component to determine whether any of GO terms were overrepresented among hDEGs [23]. The PANTHER Overrepresentation Test (release 20171205) was used to search the data against the GO database (Released 2018-02-02) to identify GO annotations overrepresented in our data when compared to a reference human genome. We used 'hierarchical view' option that groups together related classes into a "block", and orders the blocks by the largest enrichment value of any class in the block [23]. The most specific class is shown at the top of each block. The Database for Annotation, Visualization and Integrated Discovery (DAVID) tool [24] was used for KEGG-pathway enrichment analysis. Only pathways with a p-value <0.05 after Benjamini-Hochberg multiple corrections were considered.

2) Gene set enrichment analysis (GSEA) on the entire microarray dataset. Differences in GO Cellular Component terms were analyzed by also applying the so-called "second-generation" method. The advantage of this technique is that it uses information from the entire experiment (all genes, ranked according to a gene-level statistic) to generate pathway-level statistics that capture coordinated changes in the expression of genes in a pathway or gene set [25]. To this end, GSEA was conducted on data from the full chip with no prior filtering [26]. The GO gene set databases (C5.cc.v4.0) from the Molecular Signatures Database (www.broadinstitute.org/gsea/msigdb/index.jsp) were used for enrichment analysis. A thousand permutations were used to obtain the nominal *p*-value (NOM p-val). Gene sets with nominal p-value <0.05 and false discovery rate (FDR q-val) <0.25 [26], were considered to be significantly deregulated.

3) The human cell-specific gene expression database from the cell type enrichment analysis web-based tool CTen was used to predict the involvement of key cell types within candidate gene lists [27]. For each supplied gene list, the significance of cell type-specific expression was determined using the one-tailed Fisher's exact test with a Bonferroni correction across all the available cell/tissue types.

Expression validation with droplet digital polymerase chain reaction (PCR) and quantitative reverse transcription PCR

The gene expression results obtained by microarray data analysis were validated using droplet digital PCR (ddPCR) and quantitative reverse transcription polymerase chain reaction (RT-qPCR). Genes were selected based on their significance or the pathway in which they are involved. Briefly, one microgram of RNA was retro-transcribed using the High Capacity RNA-to-cDNA kit (Applied Biosystems, Foster City, CA, USA). Reactions for ddPCR assay were carried out using the QX200Droplet Generator, the QX200 Droplet Reader, the C1000 Touch Thermal Cycler, and the PX1 PCR Plate Sealer (Bio-Rad, Hercules, CA, USA) following manufacturer's instructions. Reactions were performed in duplicate using the 2× ddPCR Supermix for Probes (No dUTP) and 20x target/reference primers/probe (Bio-Rad, Supplementary Table S1). The cDNA copies/unit were quantified using the QuantaSoft Software (Bio-Rad). The expression of the following four reference genes was integrated in our experiment: *ACTB* (actin beta), *XPNPEP1* (X-prolyl aminopeptidase (aminopeptidase P1, soluble)), that was identified as a gold standard reference gene for RNA expression studies in human CNS post-mortem tissue [20], *UBE2D2* (ubiquitin-conjugating enzyme E2D 2) and *CYC1* (cytochrome c1), recently reported and validated as a stable gene useful for gene expression studies in brain tissue and neurodegenerative diseases [28]. The expression of these genes identified by microarray was comparable between sCJD and CTRL (q-value: *ACTB*=0.56, *CYC1*=0.08, *UBE2D2*=0.19, *XPNPEP1*=0.13). To achieve data normalization, cDNA copies of the target genes were adjusted by the corresponding normalization factor

(geometric mean of *ACTB, CYC1*, *UBE2D2*, and *XPNPEP1* normalization factors) [29], and final data displayed as fold change (sCJD versus CTRL). RT-qPCR reactions were carried out using the TaqMan Gene Expression Assays (Applied Biosystem, assay IDs are reported in Supplementary Table S1), according to manufacturer's instructions, on an ABI- Prism 7500 Fast Instrument (Applied Biosystem). Gene expression was normalized to *XPNPEP1* gene. Gene expression fold changes were calculated using the ΔΔCt method [30].

Western blotting

Brain tissue samples were homogenized in lysis buffer (Tris-HCl 50mM, NaCl 150mM, SDS 0.1%, Triton 1%, EDTA 1mM, pH 7.6) containing a protease inhibitor cocktail (Sigma-Aldrich, Inc. St. Luis, MO). Protein concentration was assessed by BCA assay kit (Pierce, Rockford, USA). Total lysates (20µg) were loaded into a SDS-polyacrylamide gel. Proteins were electro-transferred onto an Immobilion-P PVDF membrane (Millipore Corp., Billerica, MA). The membrane was incubated with Ab anti-VPS35 (sc-374372, Santa Cruz Biotechnology Inc., Santa Cruz, CA, 1:10000) and anti-Actin (1:10000, Sigma-Aldrich), washed and incubated with a horseradish peroxidase-conjugated secondary Ab (1:10.000, sheep anti-mouse IgG horseradish peroxidase (HRP), GE Helthcare, Little Chalfont, UK). Signals were visualized using Immobilion Western Chemiluminescent HRP substrate (Millipore Corp.) and detected by LAS-3000 (Fujifilm Co., Tokyo, Japan). Densitometric analysis was performed using the software AIDA (Image Data Analyzer v.4.15, Raytest GmbH).

Statistical analysis

To correct for multiple hypotheses, p-values were adjusted by the method of Benjamini and Hochberg or Bonferroni [31] and referred in the manuscript as q-values.

Statistical analyses on ddPCR, RT-qPCR and Western blot data were performed with SigmaPlot 12.5 (Systat Software Inc.). Depending on the data distribution, the Student's *t*-test or the Mann-Whitney test was used to detect differences between two groups. Statistical significance was set at $p/q<0.05$ unless specified otherwise.

RESULTS

Defining the transcriptional signature of sCJD

The hierarchical clustering of all analyzed genes showed that the expression profiles of most of the samples within each group were pooled together (Fig. 1a). A comparison between sCJD and controls identified 2624 differentially regulated genes with a q-value <0.05 (Supplementary Table S2). To prioritize the genes potentially involved in sCJD, we focused all subsequent analyses on those with an absolute Log_2(FC) greater than one (Supplementary Table S3). We recognized 333 highly hDEGs, of which 183 were up-regulated (fold change>2) and 150 down-regulated (fold change<0.5) (Fig. 1b, Supplementary Table S3).

To validate microarray expression data, we performed ddPCR and RT-qPCR analyses of nine selected hDEGs (CCAAT/enhancer-binding protein alpha (*CEBPA*), Colony Stimulating Factor 1 Receptor (*CSF1R*), Enolase 2 (*ENO2*), Glial fibrillary acidic protein (*GFAP*), Integrin Subunit Beta 2 (*ITGB2),* Neurofilament Medium (*NEFM*), Member RAS Oncogene Family 31 (*RAB31*), Serpin Family A Member 3 (*SERPINA3*), and TYRO Protein Tyrosine Kinase Binding Protein(*TYROBP*) genes) (Fig. 1c and Supplementary Fig. S1). All tested genes yielded results in line with microarray data.

Since large-scale transcriptional changes in tissues may be limited by changes in the proportion of constituent cell types [32], we also studied cell type-specific genes, neuronal, glial, and vascular, found by single-cell RNA sequencing [33], With this approach we demonstrated an increased expression of

genes specific to oligodendrocytes (p-value<0.001), astrocytes (p-value<0.001) and microglia (p-value=0.01), and a down-regulation of neuronal genes (p-value<0.001) (Supplementary Fig. S2). Except for microglia, median values of Log_2(FC) for each cell type subgroup were close to zero, indicating a limited effect of the change in cell type composition on global gene expression.

Biological processes alterations in sCJD

To gain insight into the biological relevance of the 333 hDEGs (Supplementary Table S3), we performed a functional enrichment GO analysis using PANTHER [23]. This analysis revealed 118 biological processes altered in sCJD (q-value<0.05) (Table 1 and Supplementary Table S4). The corresponding hDEGs were mainly associated with synaptic transmission, including GABA (q-value=0.049) and glutamate (q-value=0.005) signaling, and with the immune/inflammatory response (production of molecular mediator involved in the inflammatory response, q-value=0.04, and regulation of the immune response, q-value=0.04).

Furthermore, the dysregulation of the genes involved in the secretory pathway (q-value<0.01) suggested an alteration of the vesicle-mediated transport. Other biological processes involved included positive regulation of cellular communication (q-value<0.01), gene expression (q-value=0.03), cell morphogenesis (q-value=0.02), regulation of intracellular signal transduction (q-value<0.01), and intracellular transport (q-value<0.01). The involvement of the synaptic vesicle cycle, GABAergic synapses, and other pathways related to the immune response were also confirmed by KEGG pathway analysis (Supplementary Fig. S3).

To prioritize the biological processes underlying sCJD pathogenesis, we also applied GO functional enrichment analysis on groups of hDEGs clustered by similarity in gene expression (Supplementary Table S5). As shown in the heatmap of the 333 hDEGs (Fig. 1b), hierarchical clustering applied to hDEGs

expression values revealed six clusters, three of which (cluster one, two and three) showed significant biological process associations (q-value<0.05).

In particular, clusters one and three, including the genes mainly down-regulated in sCJD (Fig. 1b), related to synaptic transmission (Fig. 2), namely glutamate transmission in cluster one, and GABAergic signal in cluster three, whereas group two included up-regulated genes participating in several biological processes involved in the immune/inflammatory response (Fig. 1b, 2). Finally, only one GO term was found associated with two clusters. Both cluster one (q-value=0.01) and cluster two (q-value<0.01) (Supplementary Table S5) included genes involved in the regulation of vesicle-mediated transport, suggesting a complex impairment of this cellular function in sCJD.

Genes involved in synaptic vesicle cycle are down-regulated in sCJD

Synaptic dysfunction is an early cause of neurological symptoms in prion diseases since synapses represent the initial target of PrP^{Sc} deposition [35]. Accordingly, in sCJD we detected impaired neurotransmitter secretion/transport with both GO (Table 1) and KEGG pathway enrichment analyses (Supplementary Fig. S3). The most significantly altered processes were the vesicle cycling and GABAergic transmission. Notably, nine down-regulated genes (ATPase H+ Transporting V1 Subunit G2 (*ATP6V1G2*), Complexin 1 (*CPLX1*), Dynamin 1 (*DNM1*), N-Ethylmaleimide Sensitive Factor (*NSF*), Solute Carrier Family 32 Member 1 (*SLC32A1*), Syntaxin 1A (*STX1A*), Syntaxin-binding protein 1 (STXBP1), Synaptotagmin 1 (*SYT1*), Vesicle-associated membrane protein 2 (*VAMP2*), participate in different steps of the synapse vesicle cycling, including vesicle docking, priming, and fusion with the plasma membrane (Fig. 3a). These genes mainly represent components or interactors of the soluble-N-ethylmaleimide-sensitive factor attachment protein receptor (SNARE) complex that mediates vesicles - plasma membrane fusion [14].

KEGG pathway enrichment analysis also highlighted the impairment of the GABAergic synapse in sCJD (Supplementary Fig. S3). De-regulated genes (Adenylate Cyclase 1 (*ADCY1*), GABA Type A Receptor Associated Protein-Like 1 (*GABARAPL1*), Gamma-Aminobutyric Acid Type B Receptor Subunit 2 (*GABBR2*), Gamma-Aminobutyric Acid Type A Receptor Alpha1 Subunit (*GABRA1*), Gamma-Aminobutyric Acid Type A Receptor Delta Subunit (*GABRD*), Gamma-aminobutyric acid receptor subunit gamma-2 (*GABRG2*), Glutamate decarboxylase 1 (*GAD1*), Glutamate decarboxylase 2 (*GAD2),* Protein Subunit Gamma 3 (*GNG3*), N-Ethylmaleimide Sensitive Factor (*NSF*), Solute Carrier Family 32 Member 1 (*SLC32A1*), Solute carrier family 38 member 1 (*SLC38A1*)) are mainly involved in the synthesis of GABAA and GABAB receptors and in the synthesis and uptake of the neurotransmitter γ-aminobutyric acid (GABA) (Fig. 3b). These data are in agreement with previous findings that document a severe loss of neuronal inhibitory GABAergic function early in the course of TSEs [36-38].

Several pathways of the immune system are impaired in sCJD

The largest group of hDEGs (n=137) belonged to cluster 2 (Fig. 2b), which mainly included genes involved in the immune/inflammatory response (Supplementary Table S5). The functional enrichment analysis revealed an alteration of the innate immune response (q-value<0.01), the lymphocyte activation (q-value<0.01), and the production of mediators involved in the inflammatory response (q-value<0.01). To gain further insight into the immune response in sCJD, we investigated the extent of immune gene deregulation among the 333 identified hDEGs and found that 73 (21.9%) genes are annotated as involved in the immune system process (Fig. 4a, Supplementary Table S6). To identify the major cells involved in the immune response in sCJD, we then performed a cell-type enrichment analysis through the CTen platform [27] using the 73 immune-related hDEGs (Supplementary Table S6). The results suggested the involvement of different cell types, including CD14+ monocytes, CD33+ myeloid cells and BDCA4+ dendritic cells (Fig. 4b).

Previous time course studies in prion disease revealed that immune system activation precedes the appearance of spongiform change, neuronal loss and the onset of clinical signs [39]. To verify whether some immune-related-hDEGs could be involved in the early stage of human disease, we exploited the Prion Disease Database [40] that collects data related to mRNA variations spanning the interval from prion inoculation through the appearance of clinical signs in different mouse strain-prion strain combinations [8]. We found that eight of our immune system related hDEGs (Cathepsin H (*CTSH*), CCAAT/enhancer-binding protein alpha (*CEBPA*), Cluster of Differentiation 68 (*CD68*), Complement C1q B Chain (*C1QB*), Complement C1q C Chain (*C1QC*), Lymphocyte Antigen 86 (*LY86*), Serpin Family A Member 3 (*SERPINA3*), and TYRO Protein Tyrosine Kinase Binding Protein (*TYROBP*)) matched pre-clinically deregulated genes in at least four of five murine models of TSE [8] (Supplementary Fig. S4).

Vesicular trafficking is altered in sCJD

The analysis of biological process overrepresentation of hDEGs showed an impairment of the regulation of vesicle-mediated transport (Supplementary Table S5), which confirms previous data from cellular and animal models that suggest a significant membrane-trafficking alteration in sCJD [41].

While neuronal synaptic impairment and activation of the immune system are well known pathogenetic hallmarks of prion disease [39], alteration of vesicular trafficking has only recently been suggested by studies in cellular models [41, 42]. Thus, to better characterize this pathway, we performed several analyses on both the hDEGs and the whole microarray dataset.

Firstly, we performed a GO cellular component overrepresentation analysis on hDEGs (Table 2 and Supplementary Table S7). This analysis not only confirmed the deregulation of the genes involved in the synaptic vesicle (q-value=0.01) and the SNARE complex (q-value<0.01), but also identified mainly up-

regulated genes related to the endosome (q-value=0.01), lysosome (q-value=0.04), and extracellular exosome (q-value<0.01) (Table 2), highlighting the impairment of the endo-lysosomal system in sCJD. To overcome a potential bias due to hDEGs selection criteria (see Materials and Methods) we applied a GSEA analysis on all microarray data. The analysis confirmed the significant association with neuronal components such as neuron projection (q-value<0.01), with lipid raft (q-value=0.02) and lysosome (q-value=0.03). Moreover, it revealed an additional association with the Golgi apparatus (q-value=0.04) and its vesicle system (q-value=0.05) (Supplementary Table S8). Taken together, these results firmly establish the involvement of vesicular trafficking in sCJD.

The retromer core component VPS35 is down-regulated in sCJD

Recent evidence indicates that the retromer, a complex of proteins involved in the recycling transmembrane receptors from endosomes to the trans-Golgi network, is a "master conductor" of endosomal vesicle sorting and trafficking. Consequently, a retromer loss-of-function may result in significant abnormalities in the endosomal–lysosomal network, as confirmed by studies in animal models of both AD and PD [43-46]. This evidence, along with recent data suggesting an involvement of the retromer in prion disease [47, 48], led us to investigated the expression of VPS35, a key player of the retromer complex, both at gene and protein level. The latter analysis was included because previous studies revealed a predominant VPS35 defect at protein rather than RNA level [46].

Western blot analysis of brain homogenates from sCJD and controls revealed a reduced expression of protein VPS35 in sCJD brain (Fig. 5a-b, p=0.002), with no difference between MM1 and VV2 subtypes (two tale *t*-test, p-value=0.296). Interestingly, even microarray data analysis showed a trend toward a down-regulation of *VPS35* gene expression (fold change=0.74), although not statistically significant after FDR correction (p-value=0.01, q-value=0.06). The down-regulation of *VPS35* gene expression (normalized using four reference genes) was instead confirmed by ddPCR analysis (Fold Change=0.55,

p-value=0.006) (Supplementary Fig. S5). Since VPS35 is also expressed in blood cells, we verified the gene expression of seven blood-specific markers (*ALAS2*, 5'-aminolevulinate synthase 2, *HBB*, hemoglobin subunit beta, *HBA*, hemoglobin subunit alpha 2, *GYPA*, glycophorin A, *CD93*, CD93 molecule, *SPTG*, spectrin beta, erythrocytic, and *PBGD*, hydroxymethylbilane synthase, genes) [49] using microarray results. None of these genes resulted significantly differentially expressed between samples and controls, and all Log_2(FC) value were close to zero (Supplementary Table S9). Therefore, we can conclude that the different cerebral expression of VPS35 does not depend on variable amounts of contaminating blood among samples.

DISCUSSION

The identification of potential therapeutic targets remains a research priority in human prion disease, given the failure of all clinical trials conducted to date [50]. To identify the transcriptional networks modified by the disease and provide insight into the molecular pathobiology of prion disorders, we analysed the global gene expression in frontal cortex samples from sCJD patients and controls. Beside revealing several hDEGs involved in synaptic transmission and immune system function, in line with previous studies on animal and human prion diseases [7], our results demonstrate membrane trafficking abnormalities with a down-regulation of VPS35 protein, a core component of the retromer complex playing a central role in endosomal trafficking [51].

The inflammatory response is a functional pathway that is over-represented in a number of diseases, and chronic immune activation is an established feature of neurodegenerative diseases, including sCJD. Indeed, studies on both CSF, [52, 53] and brain tissue from sCJD patients [10, 54, 55] have shown an alteration of the expression of both pro- and anti-inflammatory cytokines and of immune response mediators. Accordingly, in the present study, 21.9% of hDEGs contributed to the immune response (Fig. 4a, Supplementary Table S6).

Former studies in mice demonstrated the activation of the immune system both in the pre-clinical and clinical stages of prion disease [7, 8, 56]. Among this set of genes, we confirmed the involvement of the *SERPINA3* gene, coding for a serine peptidase inhibitor (ACT), that participates in the acute phase of the inflammatory response. Notably, the finding of an up-regulation of ACT also in BSE-infected cynomolgus macaques [9] and scrapie-infected mice [8, 57], suggests a ubiquitous involvement of the protein in prion diseases.

ACT has been proposed as a biomarker for the preclinical diagnosis of prion infections because its CSF concentration raises early and increases further during disease progression in CJD, while it is only slightly elevated in AD [58]. Despite the relationship between ACT function as a trypsin inhibitor and neurodegeneration remains elusive, the protein appears to play a role in apoptotic regulation and immunity and its polymerization may accelerate the onset and enhance disease severity in AD [59].

The activation of the complement pathways is an early event in animal TSE pathogenesis [60-62]. In this regard, our finding (Supplementary Table S3) of a deregulation of C1q components (C1QB and C1QC, alias symbol C1QG), which is in line with a previous study on the immunohistochemical profile of amyloid plaques in CJD [63], endorses the role of the complement pathway in human disease. The complement system may enhance microglial activation and play a protective role by eliminating aggregated proteins, but also stimulate the production of cytokines and growth factors [64, 65], thus giving rise to a self-sustained pro-inflammatory signaling [66, 67].

Synaptic function is the second major cellular pathway impaired at a transcriptional level in sCJD (Fig. 2). This is consistent with the PrP^{C} being required for synaptic transmission [68-70], where it facilitates the release of synaptic vesicles [71]. Previous studies demonstrated an abnormal expression of synaptophysin and synapsin-1in the cerebellum of sCJD [72], and the impairment of both glutamate and GABA signaling in TSEs [34, 36-37, 73]. In murine models, impaired glutamatergic neurotransmission

and abnormal motor behaviour resulted from inefficient targeting of the voltage-gated Ca2+ channel complex to presynaptic terminals [34]. In our data set, functional analyses indicated an impairment of vesicle release and re-uptake that primarily affects glutamatergic and GABA transmission (Table 1, Fig. 2, 3a-b). Interestingly, a genome-wide association study identified a single nucleotide polymorphism in *GRM8*, encoding the mGluR8 protein, as a genetic marker associated with an increased disease risk in humans [74].

The mGluR8 protein belongs to the metabotropic glutamate receptor family, which is linked to the transduction of physiological and cytotoxic signals mediated by PrP^{C} [75], whereas mGluR1 and mGluR5 promote neurite outgrowth by interacting with PrP^{C} [76]. We found that genes involved in GABA metabolism (Fig. 3b), uptake and signaling, namely *GAD1*, *GAD2*, *GABRA1*, *GABRD*, *GABBR2*, *SLC32A1*, and *SLC38A1*, are downregulated in the frontal cortex of sCJD patients. Consistently, previous studies have shown an increase in Gabrb1 related to PrP^{Sc} formation in scrapie infected N2a cells [77] and the involvement of the GABAergic system in the brain of human and animal prion diseases [36-37, 78].

Increasing evidence indicates that a defective membrane trafficking in the endosomal/lysosomal system, involving the retromer complex, plays a significant role in the pathogenesis of neurodegenerative diseases [79-80]. Consistent with this view, our data suggest a complex dysregulation of the membrane trafficking pathway in sCJD (Table 2), which may cause synaptic dysfunction and promote the accumulation and spreading of PrP^{Sc}.

According to cellular models, PrP^{Sc} forms on the cell surface within minutes of prion exposure and is rapidly internalized into early endosomes following the PrP^{C} cycling pathway [81]. PrP^{Sc} can then be re-directed to the plasma membrane via recycling endosomes or subjected to retromer-mediated retrograde transport to the Golgi or to the late endosome/multivesicular body (LV/MVB), which are all possible sites of prion conversion [48, 82-85]. In addition, PrP^{Sc}, like PrP^{C}, can be released in the extracellular

environment, in an exosome-associated form, upon exocytic fusion of MVB with the cell surface, promoting the spread and transmission of the disease [86-89]. Lysosomes appear to be the dominant site of PrP^{Sc} degradation in the early stages of prion infection [47], while the ubiquitin-proteasome system and autophagosomes, which execute autophagy by delivering their intracellular contents to the lysosome, are involved later [47, 90]. PrP^{Sc} accumulation along the endo-lysosomal pathways interferes with post-Golgi vesicular trafficking, causing a reduced expression of proteins on the cellular surface [41]. Moreover, it impairs lysosomal maturation by lowering the rate of protein degradation, despite the increased lysosomal biogenesis [42]. Our results not only confirm the alteration of vesicle trafficking in CJD, demonstrated by the abnormal expression of genes related to the endosome, Golgi apparatus, lysosome, and extracellular vesicles, but also add new players to this dysfunctional pathway (Table 2 and Supplementary Table S8, Fig. 6). The results of previous studies on experimental prion disease showing an increased number and size of late endosomes, lysosomes and autophagic vesicles [83, 91], further support our finding. Similarly, early and late endosomes (e.g. vesicles positive for rab5 and rab7) as well as lysosomes (e.g. vescicles positive for cathepsin D and cathepsin B) were also found increased in sCJD brains [92-94].

Additionally, we demonstrated a decreased VPS35 gene and protein expression in sCJD (Fig. 5a-b, Supplementary Fig. S5), thus confirming the link between retromer dysfunction and prion disease that was recently demonstrated in a cell model, in which the knocking down of the retromer complex caused an increase in PrP^{Sc} levels [47, 48]. The retromer dysfunction would prevent the export of cargo from the endosome, impair the lysosomal activity and eventually increase the amount of PrP^{Sc} in MVB and its dissemination [95-97]. Interestingly, a retromer dysfunction, negatively affecting the endosomal-lysosomal system, has been linked to an increasing number of neurological disorders, including AD and PD [49]. In this regard, recent studies have suggested that PrP^{C} could be a receptor for oligomeric aggregates other than for PrP^{Sc} [98-99], such as alpha-synuclein and amyloid-beta [100]. As for PrP^{Sc},

PrP^C could mediate the internalization of these protein aggregates [101]. Thus, the hDEGs involving the endosomal-lysosomal pathway may represent potential novel targets of intervention aimed at limiting the spread of protein aggregates, block their toxicity, or both [102].

Limitations of the present study relate to the use of post-mortem tissue and cerebral cortex (frontal cortex only) samples in which the relative proportion between glial and neuronal cells is undefined [32]. However, by comparing our data set with that reported in the single sCJD expression profile study performed to date [10], we found that 24% of our hDEGs (n=66) was previously reported as deregulated. Moreover, this study does not provide data on gene expression during the pre-symptomatic phase of the disease. Nevertheless, the study confirms 40 hDEGs previously identified in pre-clinical disease in animal models [8]. Collectively, these data support the reliability of our results.

In conclusion, the results of our study confirm, but also extend, previous microarray expression profile data in sCJD concerning the involvement of the immune system and synaptic functions, suggesting the selective impairment of glutamatergic and GABAergic transmissions, and, above all, the involvement of the endosomal-lysosomal system. Since the latter is a pathogenic pathway linking neurodegenerative diseases such as AD, FTD and amyotrophic lateral sclerosis [51, 103-104], it might be the focus of future studies aiming to identify new targets for therapeutic interventions in neurodegenerative diseases.

AVAILABILITY OF DATA AND MATERIALS

Microarray data will be deposited in the GEO database immediately after paper acceptance. Other datasets used and analyzed during the current study are available from the corresponding author on reasonable request.

COMPLIANCE WITH ETHICAL STANDARD

The protocol of the study was approved by the Local Ethics Committee.

CONFLICT OF INTEREST

The authors declare that they have no competing interests.

AUTHORS' CONTRIBUTIONS

ABS designed and supervised whole transcriptome analysis, performed and supervised mRNA studies, analyzed, interpreted the data, and wrote the manuscript. P.C. RNA designed and supervised extraction experiments and critically reviewed the manuscript. N.M. analyzed and interpreted the data and critically reviewed the manuscript, S.B. analyzed and interpreted the data and critically reviewed the manuscript, P.F.D. and R.R designed and supervised the transcriptome analysis, and critically reviewed the manuscript, T.A. selected and prepared the samples and critically reviewed the manuscript, H.K., participated in designing the project and provided some samples, S.C. designed and supervised the study and wrote the manuscript; P.P. collected and selected the brain samples, performed all histopathological analysis, supervised the overall study and wrote the manuscript.

REFERENCES

1. Golde TE, Borchelt DR, Giasson BI, Lewis J (2013) Thinking laterally about neurodegenerative proteinopathies. J Clin Invest 123:1847-1855. doi: 10.1172/JCI66029.
2. Paulson HL (1999) Protein fate in neurodegenerative proteinopathies: polyglutamine diseases join the (mis)fold. Am J Hum Genet 64:339-345 doi:10.1086/302269.
3. Capellari S, Strammiello R, Saverioni D, Kretzschmar H, Parchi P (2011) Genetic Creutzfeldt-Jakob disease and fatal familial insomnia: insights into phenotypic variability and disease pathogenesis. Acta Neuropathol 121:21-37. doi: 10.1007/s00401-010-0760-4.
4. Ladogana A, Puopolo M, Croes EA, Budka H, Jarius C, Collins S et al (2005) Mortality from Creutzfeldt-Jakob disease and related disorders in Europe, Australia, and Canada. Neurology 64:1586-1591. doi: 10.1212/01.WNL.0000160117.56690.B2.
5. Brown P, Farrell M (2015) A practical approach to avoiding iatrogenic Creutzfeldt-Jakob disease (CJD) from invasive instruments. Infect Control Hosp Epidemiol 36:844-848. doi: 10.1017/ice.2015.53.
6. Prusiner SB (1998) Prions. Proc Natl Acad Sci U S A 95:13363-13383.
7. Basu U, Guan LL, Moore SS (2012) Functional genomics approach for identification of molecular processes underlying neurodegenerative disorders in prion diseases. Curr Genomics 13:369-378. doi: 10.2174/138920212801619223.
8. Hwang D, Lee IY, Yoo H, Gehlenborg N, Cho JH, Petritis B, et al (2009) A systems approach to prion disease. Mol Syst Biol 5:252. doi:10.1038/msb.2009.10.
9. Barbisin M, Vanni S, Schmädicke AC, Montag J, Motzkus D, Opitz L, et al (2014) Gene expression profiling of brains from bovine spongiform encephalopathy (BSE)-infected cynomolgus macaques. BMC Genomics 5:434. doi: 10.1186/1471-2164-15-434.

10. Xiang W, Windl O, Westner IM, Neumann M, Zerr I, Lederer RM, et al (2005) Cerebral gene expression profiles in sporadic Creutzfeldt-Jakob disease. Ann Neurol 58:242-57. doi: 10.1002/ana.20551.

11. Llorens F, Ansoleaga B, Garcia-Esparcia P, Zafar S, Grau-Rivera O, López-González I, et al (2013) PrP mRNA and protein expression in brain and PrP(c) in CSF in Creutzfeldt-Jakob disease MM1 and VV2. Prion 7:383-893. doi: 10.4161/pri.26416.

12. López González I, Garcia-Esparcia P, Llorens F, Ferrer I (2016) Genetic and Transcriptomic Profiles of Inflammation in Neurodegenerative Diseases: Alzheimer, Parkinson, Creutzfeldt-Jakob and Tauopathies Int J Mol Sci 17:206. doi: 10.3390/ijms17020206.

13. Burns TC, Li MD, Mehta S, Awad AJ, Morgan AA (2015) Mouse models rarely mimic the transcriptome of human neurodegenerative diseases: A systematic bioinformatics-based critique of preclinical models. Eur J Pharmacol 759:101-117. doi: 10.1016/j.ejphar.2015.03.02.

14. Durrenberger PF, Fernando S, Kashefi SN, Ferrer I, Hauw JJ, Seilhean D, et al (2010) Effects of antemortem and postmortem variables on human brain mRNA quality: a BrainNet Europe study. J Neuropathol Exp Neurol 69:70-81. doi: 10.1097/NEN.0b013e3181c7e32f.

15. Twine NA, Janitz K, Wilkins MR, Janitz M (2011) Whole transcriptome sequencing reveals gene expression and splicing differences in brain regions affected by Alzheimer's disease. PLoS One 6:e16266. doi: 10.1371/journal.pone.0016266.

16. Parchi P, de Boni L, Saverioni D, Cohen ML, Ferrer I, Gambetti P, et al (2012) Consensus classification of human prion disease histotypes allows reliable identification of molecular subtypes: an inter-rater study among surveillance centres in Europe and USA. Acta Neuropathol 124:517-529. doi: 10.1007/s00401-012-1002-8.

17. Parchi P, Notari S, Weber P, Schimmel H, Budka H, Ferrer I, et al (2009) Inter-laboratory assessment of PrPSc typing in creutzfeldt-jakob disease: a Western blot study within the NeuroPrion Consortium. Brain Pathol 19:384-391. doi: 10.1111/j.1750-3639.2008.00187.x.

18. Montine TJ, Phelps CH, Beach TG, Bigio EH, Cairns NJ, Dickson DW, Duyckaerts C, Frosch MP, Masliah E, Mirra SS, Nelson PT, Schneider JA, Thal DR, Trojanowski JQ, Vinters HV, Hyman BT; National Institute on Aging; Alzheimer's Association (2012) National Institute on Aging-Alzheimer's Association guidelines for the neuropathologic assessment of Alzheimer's disease: a practical approach. Acta Neuropathol 123:1-11. doi: 10.1007/s00401-011-0910-3.

19. Parchi P, Giese A, Capellari S, Brown P, Schulz-Schaeffer W, Windl O, Zerr I, Budka H, Kopp N, Piccardo P, Poser S, Rojiani A, Streichemberger N, Julien J, Vital C, Ghetti B, Gambetti P, Kretzschmar H (1999) Classification of sporadic Creutzfeldt-Jakob disease based on molecular and phenotypic analysis of 300 subjects. Ann Neurol 46:224-233.

20. Durrenberger PF, Fernando FS, Magliozzi R, Kashefi SN, Bonnert TP, Ferrer I, et al (2012) Selection of novel reference genes for use in the human central nervous system: a BrainNet Europe Study. Acta Neuropathol 124:893-903. doi: 10.1007/s00401-012-1027-z.

21. Bartoletti-Stella A, Gasparini L, Giacomini C, Corrado P, Terlizzi R, Giorgio E, et al (2015) Messenger RNA processing is altered in autosomal dominant leukodystrophy. Hum Mol Genet 24:2746-2756. doi: 10.1093/hmg/ddv034.

22. Mlecnik B, Galon J, Bindea G (2018) Comprehensive functional analysis of large lists of genes and proteins. J Proteomics 16;171:2-10. doi: 10.1016/j.jprot.2017.03.016.

23. Mi H, Huang X, Muruganujan A, Tang H, Mills C, Kang D, et al (2017) PANTHER version 11: expanded annotation data from Gene Ontology and Reactome pathways, and data analysis tool enhancements. Nucleic Acids Res 45:D183-D189. doi: 10.1093/nar/gkw1138.

24. Huang DW, Sherman BT, Lempicki RA (2009) Systematic and integrative analysis of large gene lists using DAVID Bioinformatics Resources. Nat Protoc 4:44-57. doi: 10.1038/nprot.2008.211.

25. Davis MJ, Ragan MA (2013) Understanding cellular function and disease with comparative pathway analysis. Genome Med 5:64. doi: 10.1186/gm468.

26. Subramanian A, Tamayo P, Mootha VK, Mukherjee S, Ebert BL, Gillette MA et al (2005) Gene set enrichment analysis: a knowledge-based approach for interpreting genome-wide expression profiles. Proc Natl Acad Sci U S A 102:15545-15550. doi:10.1073/pnas.0506580102.

27. Shoemaker J.E., Lopes T.J.S., Ghosh S., Matsuoka Y., Kawaoka Y, Kitano H et al (2012) CTen: a web-based platform for identifying enriched cell types from heterogeneous microarray data. BMC Genomics 13:460. doi: 10.1186/1471-2164-13-460.

28. Rydbirk R, Folke J, Winge K, Aznar S, Pakkenberg B, Brudek T (2016) Assessment of brain reference genes for RT-qPCR studies in neurodegenerative diseases. Sci Rep 6:37116. doi: 10.1038/srep37116.

29. Millier MJ, Stamp LK, Hessian PA (2017) Digital-PCR for gene expression: impact from inherent tissue RNA degradation. Sci Rep 7:17235. doi:10.1038/s41598-017-17619-0.

30. Livak KJ, Schmittgen TD (2001) Analysis of relative gene expression data using real-time quantitative PCR and the 2(-Delta Delta C(T)) Method. Methods 25:402-408 doi: 10.1006/meth.2001.1262.

31. Storey JD, Tibshirani R (2003) Statistical significance for genomewide studies. Proc Natl Acad Sci U S A 100:9440-9445. doi: 10.1073/pnas.1530509100.

32. Ramaker RC, Bowling KM, Lasseigne BN, Hagenauer MH, Hardigan AA, Davis NS, et al (2017) Post-mortem molecular profiling of three psychiatric disorders. Genome Med 9:72. doi: 10.1186/s13073-017-0458-5.

33. Darmanis S, Sloan SA, Zhang Y, Enge M, Caneda C, Shuer LM et al (2015) A survey of human brain transcriptome diversity at the single cell level. Proc Natl Acad Sci U S A 112:7285-7290. doi: 10.1073/pnas.1507125112.

34. Senatore A, Restelli E, Chiesa R (2013) Synaptic dysfunction in prion diseases: a trafficking problem? Int J Cell Biol 2013:543803. doi: 10.1155/2013/543803.

35. Bombardier JP, Munson M (2015) Three steps forward, two steps back: mechanistic insights into the assembly and disassembly of the SNARE complex. Curr Opin Chem Biol 29:66-71. doi: 10.1016/j.cbpa.2015.10.003.

36. Bouzamondo-Bernstein E, Hopkins SD, Spilman P, Uyehara-Lock J, Deering C, Safar J, et al (2004) The neurodegeneration sequence in prion diseases: evidence from functional, morphological and ultrastructural studies of the GABAergic system. J Neuropathol Exp Neurol 63:882-899.

37. Guentchev M, Groschup MH, Kordek R, Liberski PP, Budka H (1998) Severe, early and selective loss of a subpopulation of GABAergic inhibitory neurons in experimental transmissible spongiform encephalopathies. Brain Pathol 8:615-623.

38. Trifilo MJ, Sanchez-Alavez M, Solforosi L, Bernard-Trifilo J, Kunz S, McGavern D, et al (2008) Scrapie-induced defects in learning and memory of transgenic mice expressing anchorless prion protein are associated with alterations in the gamma aminobutyric acid-ergic pathway. J Virol 82:9890-9899. doi: 10.1128/JVI.00486-08.

39. Aguzzi A, Zhu C (2017) Microglia in prion diseases. J Clin Invest 127:3230-3239. doi: 10.1172/JCI90605.

40. Gehlenborg N, Hwang D, Lee IY, Yoo H, Baxter D, Petritis B, et al (2009) The Prion Disease Database: a comprehensive transcriptome resource for systems biology research in prion diseases. Database (Oxford) 2009:bap011. doi: 10.1093/database/bap011.

41. Uchiyama K, Muramatsu N, Yano M, Usui T, Miyata H, Sakaguchi S (2013) Prions disturb post-Golgi trafficking of membrane proteins. Nat Commun 4:1846. doi: 10.1038/ncomms2873.

42. Shim SY, Karri S, Law S, Schatzl HM, Gilch S (2016) Prion infection impairs lysosomal degradation capacity by interfering with rab7 membrane attachment in neuronal cells. Sci Rep 6:21658. doi: 10.1038/srep21658.

43. MacLeod DA, Rhinn H, Kuwahara T, Zolin A, Di Paolo G, McCabe BD, Marder KS, Honig LS, Clark LN, Small SA, Abeliovich A (2013) RAB7L1 interacts with LRRK2 to modify intraneuronal protein sorting and Parkinson's disease risk. Neuron 77:425-439. doi: 10.1016/j.neuron.2012.11.033.

44. Wen L, Tang FL, Hong Y, Luo SW, Wang CL, He W, Shen C, Jung JU, Xiong F, Lee DH, Zhang QG, Brann D, Kim TW, Yan R, Mei L, Xiong WC (2011) VPS35 haploinsufficiency increases Alzheimer's disease neuropathology. J Cell Biol 195:765-79. doi: 10.1083/jcb.201105109.

45. Muhammad A, Flores I, Zhang H, Yu R, Staniszewski A, Planel E, Herman M, Ho L, Kreber R, Honig LS, Ganetzky B, Duff K, Arancio O, Small SA (2008) Retromer deficiency observed in Alzheimer's disease causes hippocampal dysfunction, neurodegeneration, and Abeta accumulation. Proc Natl Acad Sci U S A 105:7327-32. doi: 10.1073/pnas.0802545105.

46. Small SA, Kent K, Pierce A, Leung C, Kang MS, Okada H, Honig L, Vonsattel JP, Kim TW. (2005) Model-guided microarray implicates the retromer complex in Alzheimer's disease. Ann Neurol 2005 58:909-19.

47. Goold R, McKinnon C, Rabbanian S, Collinge J, Schiavo G, Tabrizi SJ (2013) Alternative fates of newly formed PrPSc upon prion conversion on the plasma membrane. J Cell Sci 126:3552-3562. doi: 10.1242/jcs.120477.

48. Yim YI, Park BC, Yadavalli R, Zhao X, Eisenberg E, Greene LE (2015) The multivesicular body is the major internal site of prion conversion. J Cell Sci 128:1434-1443. doi:10.1242/jcs.165472.

49. Takada LT, Geschwind MD (2013) Prion diseases. Semin Neurol 33:348-856. doi: 10.1055/s-0033-1359314.

50. Zhao H, Wang C, Yao L, Lin Q, Xu X, Hu L, Li W (2017) Identification of aged bloodstains through mRNA profiling: Experiments results on selected markers of 30- and 50-year-old samples. Forensic Sci Int 272:e1-e6. doi:10.1016/j.forsciint.2017.01.006.

51. Small SA, Petsko GA (2015) Retromer in Alzheimer disease, Parkinson disease and other neurological disorders. Nat Rev Neurosci 16:126-132. doi: 10.1038/nrn3896.

52. Sharief MK, Green A, Dick JP, Gawler J, Thompson EJ (1999) Heightened intrathecal release of proinflammatory cytokines in Creutzfeldt-Jakob disease. Neurology 52:1289-1291.

53. Stoeck K, Bodemer M, Zerr I (2006) Pro- and anti-inflammatory cytokines in the CSF of patients with Creutzfeldt-Jakob disease. J Neuroimmunol 172:175-181. doi: 10.1016/j.jneuroim.2005.10.008.

54. Llorens F, López-González I, Thüne K, Carmona M, Zafar S, Andréoletti O, et al (2014) Subtype and regional-specific neuroinflammation in sporadic creutzfeldt-jakob disease. Front Aging Neurosci 6:198. doi: 10.3389/fnagi.2014.00198.

55. Shi Q, Chen LN, Zhang BY, Xiao K, Zhou W, Chen C, et al (2015) Proteomics analyses for the global proteins in the brain tissues of different human prion diseases. Mol Cell Proteomics 14:854-869. doi: 10.1074/mcp.M114.038018.

56. Booth S, Bowman C, Baumgartner R, Sorensen G, Robertson C, Coulthart M, et al (2004) Identification of central nervous system genes involved in the host response to the scrapie agent during preclinical and clinical infection. J Gen Virol 85:3459-3471.

57. Xiang W, Hummel M, Mitteregger G, Pace C, Windl O, Mansmann U, et al (2007) Transcriptome analysis reveals altered cholesterol metabolism during the neurodegeneration in mouse scrapie model. J Neurochem 102:834-847. doi:10.1111/j.1471-4159.2007.04566.x.

58. Vanni S, Moda F, Zattoni M, Bistaffa E, De Cecco E, Rossi M, et al (2017) Differential overexpression of SERPINA3 in human prion diseases. Sci Rep 7:15637. doi: 10.1038/s41598-017-15778 8.

59. Heit C, Jackson BC, McAndrews M, Wright MW, Thompson DC, Silverman GA, et al (2013) Update of the human and mouse SERPIN gene superfamily. Hum Genomics 7:22. doi: 10.1186/1479-7364-7-22.

60. Cardone F, Pocchiari M (2001) A role for complement in transmissible spongiform encephalopathies. Nat Med 7:410-411. doi: 10.1038/86469

61. Klein MA, Kaeser PS, Schwarz P, Weyd H, Xenarios I, Zinkernagel RM (2001) Complement facilitates early prion pathogenesis. Nat Med 7:488-492 doi: 10.1038/86567.

62. Mitchell DA, Kirby L, Paulin SM, Villiers CL, Sim RB (2007) Prion protein activates and fixes complement directly via the classical pathway: implications for the mechanism of scrapie agent propagation in lymphoid tissue. Mol Immunol 44:2997-3004. doi: 10.1016/j.molimm.2006.12.027.

63. Kovacs GG, Gasque P, Ströbel T, Lindeck-Pozza E, Strohschneider M, Ironside JW, et al (2004) Complement activation in human prion disease. Neurobiol Dis 15:21-28.

64. Bonifati DM, Kishore U (2007) Role of complement in neurodegeneration and neuroinflammation. Mol Immunol 44:999-1010.

65. Mabbott NA, Bruce ME, Botto M, Walport MJ, Pepys MB (2001) Temporary depletion of complement component C3 or genetic deficiency of C1q significantly delays onset of scrapie. Nat Med 7:485-487. doi:10.1038/86562.

66. Anisman H, Gibb J, Hayley S (2008) Influence of continuous infusion of interleukin-1beta on depression-related processes in mice: corticosterone, circulating cytokines, brain monoamines, and cytokine mRNA expression. Psychopharmacology (Berl) 199:231-244. doi: 10.1007/s00213-008-1166-z.

67. Frankola KA, Greig NH, Luo W, Tweedie D (2011) Targeting TNF-α to elucidate and ameliorate neuroinflammation in neurodegenerative diseases. CNS Neurol Disord Drug Targets 10:391-403. doi: 10.2174/187152711794653751.

68. Mallucci GR, Ratté S, Asante EA, Linehan J, Gowland I, Jefferys JG, et al (2002) Post-natal knockout of prion protein alters hippocampal CA1 properties, but does not result in neurodegeneration. EMBO J 21:202-210. doi:10.1093/emboj/21.3.202.

69. Rangel A, Madroñal N, Gruart A, Gavín R, Llorens F, Sumoy L, et al (2009) Regulation of GABA(A) and glutamate receptor expression, synaptic facilitation and long-term potentiation in the hippocampus of prion mutant mice. PLoS One 4:e7592. doi: 10.1371/journal.pone.0007592.

70. Rincon-Limas DE, Casas-Tinto S, Fernandez-Funez P (2010) Exploring prion protein biology in flies: genetics and beyond. Prion 4:1-8.

71. Robinson SW, Nugent ML, Dinsdale D, Steinert JR (2014) Prion protein facilitates synaptic vesicle release by enhancing release probability. Hum Mol Genet 23:4581-4596. doi: 10.1093/hmg/ddu17.

72. Ferrer I (2002) Synaptic pathology and cell death in the cerebellum in Creutzfeldt-Jakob disease. Cerebellum 1:213-222. doi: 10.1080/14734220260418448.

73. Ferrer I, Puig B (2003) GluR2/3, NMDAepsilon1 and GABAA receptors in Creutzfeldt-Jakob disease. Acta Neuropathol 106:311-318. doi: 10.1007/s00401-003-0732-z.

74. Sanchez-Juan P, Bishop MT, Kovacs GG, Calero M, Aulchenko YS, Ladogana A, et al (2015) A genome wide association study links glutamate receptor pathway to sporadic Creutzfeldt-Jakob disease risk. PLoS One doi:10.1371/journal.pone.0123654.

75. Um JW, Kaufman AC, Kostylev M, Heiss JK, Stagi M, Takahashi H, et al (2013) Metabotropic glutamate receptor 5 is a coreceptor for Alzheimer aβ oligomer bound to cellular prion protein. Neuron 79:887-902. doi: 10.1016/j.neuron.2013.06.036

76. Beraldo FH, Arantes CP, Santos TG, Machado CF, Roffe M, Hajj GN, et al (2011) Metabotropic glutamate receptors transduce signals for neurite outgrowth after binding of the prion protein to laminin γ1 chain. FASEB J 25:265-279. doi: 10.1096/fj.10-161653.

77. Kimura T, Ishikawa K, Sakasegawa Y, Teruya K, Sata T, Schätzl H, et al (2010) GABAA receptor subunit beta1 is involved in the formation of protease-resistant prion protein in prion-infected neuroblastoma cells. FEBS Lett 584:1193-1198. doi: 10.1016/j.febslet.2010.02.029.

78. Pocchiari M, Masullo C, Lust WD, Gibbs CJ Jr, Gajdusek DC (1985) Isonicotinic hydrazide causes seizures in scrapie-infected hamsters with shorter latency than in control animals: a possible GABAergic defect. Brain Res 326:117-1123.

79. Abeliovich A, Gitler AD (2016) Defects in trafficking bridge Parkinson's disease pathology and genetics. Nature 539:207-216. doi: 10.1038/nature20414.

80. Schreij AM, Fon EA, McPherson PS (2016) Endocytic membrane trafficking and neurodegenerative disease. Cell Mol Life Sci 73:1529-1545. doi: 10.1007/s00018-015-2105-x.

81. Campana V, Sarnataro D, Zurzolo C (2005) The highways and byways of prion protein trafficking. Trends Cell Biol 15:102-111. doi:10.1016/j.tcb.2004.12.002.

82. Béranger F, Mangé A, Goud B, Lehmann S (2002) Stimulation of PrP(C) retrograde transport toward the endoplasmic reticulum increases accumulation of PrP(Sc) in prion-infected cells. J Biol Chem 277:38972-38977. DOI:10.1074/jbc.M205110200.

83. Borchelt DR, Taraboulos A, Prusiner SB (1992) Evidence for synthesis of scrapie prion proteins in the endocytic pathway. J Biol Chem 267:16188-16199.

84. Magalhães AC, Baron GS, Lee KS, Steele-Mortimer O, Dorward D, Prado MA, et al (2005) Uptake and neuritic transport of scrapie prion protein coincident with infection of neuronal cells. J Neurosci 25:5207-5216. doi:10.1523/JNEUROSCI.0653-05.2005.

85. Marijanovic Z, Caputo A, Campana V, Zurzolo C (2009) Identification of an intracellular site of prion conversion. PLoS Pathog 5:e1000426. doi: 10.1371/journal.ppat.1000426.

86. Aguzzi A, Rajendran L (2009) The transcellular spread of cytosolic amyloids, prions, and prionoids. Neuron 64:783-790. doi: 10.1016/j.neuron.2009.12.016.

87. Frost B, Diamond MI (2010) Prion-like mechanisms in neurodegenerative diseases. Nat Rev Neurosci 11:155-159. doi: 10.1038/nrn2786.

88. Liu S, Hossinger A, Göbbels S, Vorberg IM (2017) Prions on the run: How extracellular vesicles serve as delivery vehicles for self-templating protein aggregates. Prion 11:98-112. doi:10.1080/19336896.2017.1306162.

89. Raposo G, Stoorvogel W (2013) Extracellular vesicles: exosomes, microvesicles, and friends. J Cell Biol 200:373-383. doi: 10.1083/jcb.201211138.

90. Hu YB, Dammer EB, Ren RJ, Wang G (2015) The endosomal-lysosomal system: from acidification and cargo sorting to neurodegeneration. Transl Neurodegener 4:18. doi: 10.1186/s40035-015-0041-1.

91. Boellaard JW, Kao M, Schlote W, Diringer H (1991) Neuronal autophagy in experimental scrapie. Acta Neuropathol 82:225-228.

92. Kovács GG, Gelpi E, Ströbel T, Ricken G, Nyengaard JR, Bernheimer H, et al (2007) Involvement of the endosomal-lysosomal system correlates with regional pathology in Creutzfeldt-Jakob disease. J Neuropathol Exp Neurol 66:628-36.

93. Liberski PP, Sikorska B, Hauw JJ, Kopp N, Streichenberger N, Giraud P et al (2010) Ultrastructural characteristics (or evaluation) of Creutzfeldt-Jakob disease and other human transmissible spongiform encephalopathies or prion diseases. Ultrastruct Pathol 34:351-361. doi: 10.3109/01913123.2010.491175.

94. Zafar S, Younas N, Correia S, Shafiq M, Tahir W, Schmitz M (2017) Strain-Specific Altered Regulatory Response of Rab7a and Tau in Creutzfeldt-Jakob Disease and Alzheimer's Disease. Mol Neurobiol 54:697-709. doi: 10.1007/s12035-016-9694-8.

95. Gouras GK (2013) Convergence of Synapses, Endosomes, and Prions in the Biology of Neurodegenerative Diseases. Int J Cell Biol 2013:141083. doi: 10.1155/2013/14108.

96. Guo BB, Bellingham SA, Hill AF (2016) Stimulating the Release of Exosomes Increases the Intercellular Transfer of Prions. J Biol Chem 291:5128-5137. doi: 10.1074/jbc.M115.684258.

97. Hasegawa T, Sugeno N, Kikuchi A, Baba T, Aoki M (2017) Membrane Trafficking Illuminates a Path to Parkinson's Disease. Tohoku J Exp Med 242:63-76. doi: 10.1620/tjem.242.63.

98. Aulić S, Masperone L, Narkiewicz J, Isopi E, Bistaffa E, Ambrosetti E, et al (2017) α-Synuclein Amyloids Hijack Prion Protein to Gain Cell Entry, Facilitate Cell-to-Cell Spreading and Block Prion Replication. Sci Rep 7:10050. doi: 10.1038/s41598-017-10236-x.

99. Fluharty BR, Biasini E, Stravalaci M, Sclip A, Diomede L, Balducci C, et al (2013) An N-terminal fragment of the prion protein binds to amyloid-β oligomers and inhibits their neurotoxicity in vivo. J Biol Chem 288:7857-7866. doi: 10.1074/jbc.M112.423954.

100. Resenberger UK, Winklhofer KF, Tatzelt J (2011) Neuroprotective and neurotoxic signaling by the prion protein 305:101-119. doi: 10.1007/128_2011_160.

101. Holmes BB, DeVos SL, Kfoury N, Li M, Jacks R, Yanamandra K, et al (2013) Heparan sulfate proteoglycans mediate internalization and propagation of specific proteopathic seeds. Proc Natl Acad Sci U S A 110:E3138-3147. doi: 10.1073/pnas.1301440110.

102. Ballmer BA, Moos R, Liberali P, Pelkmans L, Hornemann S, Aguzzi A (2017) Modifiers of prion protein biogenesis and recycling identified by a highly parallel endocytosis kinetics assay. J Biol Chem. 292:8356-8368. doi: 10.1074/jbc.M116.773283.

103. Nixon RA (2013) The role of autophagy in neurodegenerative disease. Nat Med 1:983-997. doi: 10.1038/nm.3232.

104. Schneider JL, Cuervo AM (2014) Autophagy and human disease: emerging themes. Curr Opin Genet Dev 26:16-23 doi: 10.1016/j.gde.2014.04.00.

105. Babicki S, Arndt D, Marcu A, Liang Y, Grant JR, Maciejewski A, et al (2016) Heatmapper: web-enabled heat mapping for all. Nucleic Acids Res 8;44:W147-53. doi: 10.1093/nar/gkw419.

FIGURE LEGENDS

Fig. 1 Genome-wide expression analysis in sCJD frontal cortex

a: Hierarchical clustering (Pearson correlation, pairwise average-linkage) [105] based on the expression values of all 18.000 genes detected by BeadChip Illumina after normalization. **b**: HeatMap (Heat-Mapper [105]) representing the 333 highly deregulated genes (hDEGs) in sCJD patients (n = 10) vs controls (n = 10) at q-value<0.05 and Log(FC)>|1|. 183 genes were up-regulated (red), and 150 down-regulated (green). Genes are clustered by samples class (Control or sCJD) and by the similarity in gene expression.

Clustering yielded six hDEGs clusters. hDEGs belonging to each cluster are listed in the Supplementary Table S5. **c**: Validation of microarray gene expression levels by ddPCR, genes analyzed: CCAAT/enhancer-binding protein alpha, *CEBPA*, Colony Stimulating Factor 1 Receptor, *CSF1R*, Enolase 2 *ENO2*, Glial fibrillary acidic protein, *GFAP*, Integrin Subunit Beta 2, *ITGB2*, Neurofilament Medium *NEFM*, Member RAS Oncogene Family 31, *RAB31*, Serpin Family A Member 3, *SERPINA3*, and TYRO Protein Tyrosine Kinase Binding Protein, *TYROBP*. Data obtained from microarray profiling (gray bars) were comparable to those obtained by ddPCR (blue bars). Data are expressed as fold change (sCJD versus CTRL) normalized with the expression of four reference genes: *ACTB* (actin beta), *XPNPEP1* (X-prolyl aminopeptidase (aminopeptidase P1, soluble)), *UBE2D2* (ubiquitin-conjugating enzyme E2D 2) and *CYC1* (cytochrome c1). On the Y-axis, bars represent fold change as multiple of the mean value in controls (arbitrarily set to one) while error bars represent standard deviation. On the X-axis the tested genes. The expression of target genes (normalized on *XPNPEP1* gene expression level) was also analyzed by RT-qPCR (Supplementary Fig. S1).

CTRL, controls; FC, fold change; hDEGs, higthly differentially expressed genes; RT-qPCR, reverse transcription- quantitative polymerase chain reaction; sCJD, sporadic Creutzfeldt-Jakob disease.

Fig. 2 Functional analysis of hDEGs

Gene Ontology biological process analysis performed on clusters of hDEGs grouped for similar expression value obtained by the PANTHER tool [23]. The analysis has been performed considering the hierarchical order of GO terms and only the most specific GO terms are shown. On the X-axis, bars represent the $-\text{Log}_{10}$ of the q-value resulting from the overrepresentation test (Test Type: Binomial, Bonferroni correction for multiple testing). On the Y-axis the most specific significant GO. The complete list of significant GO terms is listed in the Supplementary Table S5.

GO, gene ontology; hDEGs, highly differentially expressed genes.

Fig. 3 Gene alterations related to the cycle of synaptic vesicles and GABAergic synapse in sCJD

a: HeatMap (performed by using Heat-Mapper tool [105]) representing the 10 hDEGs (*ATP6V0E1*, ATPase H+ transporting V0 subunit e1; *ATP6V1G2*, ATPase H+ Transporting V1 Subunit G2; *CPLX1*, Complexin 1; *DNM1*, Dynamin 1; *NSF*, N-Ethylmaleimide Sensitive Factor; *SLC32A1*, Solute Carrier Family 32 Member 1; *STX1A*, Syntaxin 1A; *STXBP1*, Syntaxin binding protein 1; *SYT1*, Synaptotagmin 1; *VAMP2*, Vesicle-associated membrane protein 2) linked to the KEGG pathway "synaptic vesicle cycle". hDEGs up-regulated are shown in red down-regulated in green. **b:** HeatMap (performed by using Heat-Mapper tool [105]) representing the 12 hDEGs (*ADCY1*, Adenylate Cyclase 1; *GABARAPL1*, GABA Type A Receptor Associated Protein Like 1; *GABBR2*, Gamma-Aminobutyric Acid Type B Receptor Subunit 2; *GABRA1*, Gamma-Aminobutyric Acid Type A Receptor Alpha1 Subunit; *GABRD*, Gamma-Aminobutyric Acid Type A Receptor Delta Subunit; *GABRG2*, Gamma-aminobutyric acid receptor subunit gamma-2; *GAD1*, Glutamate decarboxylase 1; *GAD2*, Glutamate decarboxylase 2; *GNG3*, Protein Subunit Gamma 3; *NSF*, N-Ethylmaleimide Sensitive Factor; *SLC32A1*, Solute Carrier Family 32 Member 1; *SLC38A1*, Solute carrier family 38 member 1) linked to KEGG pathway "GABAergic synapse". All these hDEGs were down-regulated (green) in sCJD.

hDEGs, highly differentially expressed genes.

Fig. 4 Immune response in sCJD

a: HeatMap (performed by using Heat-Mapper tool [105]) representing the 73 hDEGs included in the biological process term "immune system process" [23] obtained by overrepresentation analysis test performed by PANTHER tool. hDEGs down-regulated in sCJD are shown in green, up-regulated in red. hDEGs symbols and names are listed in the Supplementary Table S6. **b:** Cell-type enrichment analysis of hDEGs involved in "immune system process" performed using the tool C-Ten [27]. Cell-types/organs with a q-value<0.05 and an enrichment score>2 are shown in the Y-axis, on the X-axis, bars represent the enrichment score, corresponding to $-\text{Log}_{10}$ Benjamini-Hochberg adjusted P-value [27].

CTRL, controls; hDEGs, highly differentially expressed genes; sCJD, sporadic Creutzfeldt-Jakob disease.

Fig. 5 The retromer core component VPS35 expression in sCJD

a: Representative image of VPS35 protein expression by western blot analysis of 4 CTRL and 4 sCJD samples. Beta-actin was used as housekeeping protein for normalization. **b:** Box-plot of VPS35/beta actin protein expression ratio relative to western blot analysis performed on 7 CTRL and 8 sCJD brain homogenate (Mann-Whitney test). Densitometric analysis was performed using the software AIDA (Image Data Analyzer v.4.15, Raytest GmbH). Relative molecular masses are expressed in kDa. Gene expression analysis of VPS35 is shown in the Supplementary Fig. S5.

CTRL, controls; hDEGs, highly differentially expressed genes; sCJD, sporadic Creutzfeldt-Jakob disease, VPS35, Vacuolar protein sorting-associated protein 35.

Fig. 6 Vesicle trafficking alteration in sCJD

Vesicle deregulated genes (reported in the table) involved in vesicle trafficking identified in this study. Membrane raft, endosome, lysosome, and extracellular vesicle related genes were mainly up-regulated, while clathrin-coated vesicle and Golgi genes resulted down-regulate. Bars below cellular compartments reported the percentage of up-regulated (red) down-regulated genes (green). The down-regulation of the retromer core protein VPS35 (Fig. 5a-b) suggests an impairment of the retrograde transport of the PrP^{C} and the lysosomal enzymes leading to an inefficient lysosomal activity. Accordingly, in sCJD, PrP^{Sc} accumulates in multivesicular body and, due to an inefficient degradative pathway (lysosomal and

proteasome-mediated), may be release in the extracellular space thought the exosomes, favoring its dissemination.

Table 1 Biological process GO terms altered in sCJD frontal cortex.

GO biological process complete	Fold Enrichment	q-value	% up-regulated hDEGs
synaptic transmission, GABAergic (GO:0051932)	36.33	4.78E-02	0
production of molecular mediator involved in inflammatory response (GO:0002532)	21.19	4.22E-02	100
glutamate secretion (GO:0014047)	15.34	4.49E-03	28.57
positive regulation of regulated secretory pathway (GO:1903307)	10.82	9.30E-03	50
L-amino acid transport (GO:0015807)	9.38	6.39E-03	55.55
calcium ion regulated exocytosis (GO:0017156)	7.84	2.73E-02	22.22
vesicle-mediated transport in synapse (GO:0099003)	7.06	1.89E-03	8.33
synaptic vesicle cycle (GO:0099504)	6.99	6.67E-03	9.09
neurotransmitter secretion (GO:0007269)	6.86	8.07E-03	9.09
cellular response to metal ion (GO:0071248)	5.78	2.08E-03	78.57
cellular response to external stimulus (GO:0071496)	3.84	1.52E-02	77.78
regulation of intracellular transport (GO:0032386)	3.50	8.86E-03	47.62
neuron projection development (GO:0031175)	3.14	2.58E-04	37.71
import into cell (GO:0098657)	3.11	1.13E-04	63.64
myeloid cell activation involved in immune response (GO:0002275)	3.09	7.91E-03	92

regulation of cell activation (GO:0050865)	2.88	1.74E-02	80.77
cellular response to oxygen-containing compound (GO:1901701)	2.81	5.05E-05	65
cell morphogenesis (GO:0000902)	2.78	1.35E-02	42.86
response to lipid (GO:0033993)	2.52	1.35E-02	81.82
response to drug (GO:0042493)	2.51	4.52E-03	63.89
positive regulation of multicellular organismal process (GO:0051240)	2.44	2.72E-06	72.41
cellular response to endogenous stimulus (GO:0071495)	2.34	4.23E-03	60.98
positive regulation of cellular component organization (GO:0051130)	2.31	3.01E-03	65.12
cellular response to organic substance (GO:0071310)	2.28	4.54E-08	67.53
regulation of immune response (GO:0050776)	2.24	4.27E-02	81.08
positive regulation of signaling (GO:0023056)	2.04	5.43E-03	64.81
positive regulation of cell communication (GO:0010647)	2.01	1.09E-02	66.04
regulation of intracellular signal transduction (GO:1902531)	1.94	1.49E-02	70.18
gene expression (GO:0010467)	.49	1.42E-02	50
nucleic acid metabolic process (GO:0090304)	.44	5.70E-04	51.72

Overrepresented GO Biological Process categories yielded by the analysis on the 333 hDEGs, with a q-value (Bonferroni correction) <0.05 and a fold enrichment >2 or <0.5 [23]. The most specific GO biological process terms are shown (see materials and methods); the complete list of significant GO terms (q-value<0.05) is listed in the Supplementary Table S4. Test Type: Binomial, Bonferroni correction for multiple testing.

Table 2. Cellular component GO terms altered in sCJD frontal cortex.

GO biological process complete	Fold Enrichment	q-value	% up-regulated hDEGs
clathrin-sculpted gamma-aminobutyric acid transport vesicle membrane (GO:0061202)	39.73	3.11E-04	0
neurofilament (GO:0005883)	25.43	2.99E-02	25
integral component of synaptic vesicle membrane (GO:0030285)	18.70	1.20E-02	0
MHC class II protein complex (GO:0042613)	16.73	2.04E-02	100
SNARE complex (GO:0031201)	9.25	4.57E-03	12.5
terminal bouton (GO:0043195)	7.82	1.52E-02	12.5
myelin sheath (GO:0043209)	7.10	7.81E-08	21.05
tertiary granule membrane (GO:0070821)	6.97	3.45E-02	87.5
postsynaptic density (GO:0014069)	5.53	1.21E-05	22.22
membrane raft (GO:0045121)	4.17	1.75E-04	70
receptor complex (GO:0043235)	3.92	4.49E-04	75
synaptic membrane (GO:0097060)	3.85	2.25E-03	11.11
cell body (GO:0044297)	3.13	9.66E-04	36
cell junction (GO:0030054)	2.90	1.27E-09	41.07

somatodendritic compartment (GO:0036477)	2.72	1.37E-03	23.33
perinuclear region of cytoplasm (GO:0048471)	2.56	1.42E-02	59.26
lysosome (GO:0005764)	2.48	3.61E-02	88.46
endosome (GO:0005768)	2.32	1.49E-02	71.86
integral component of plasma membrane (GO:0005887)	2.31	2.38E-06	57.63
extracellular exosome (GO:0070062)	1.94	1.99E-06	67.47

Overrepresented GO Cellular Component categories yielded by the analysis on the 333 hDEGs, with a q-value (Bonferroni correction) <0.05 [23]. The most specific GO biological process terms are shown (see materials and methods); the complete list of significant GO terms (q-value<0.05) is listed in the Supplementary Table S7. Test Type: Binomial, Bonferroni correction for multiple testing.

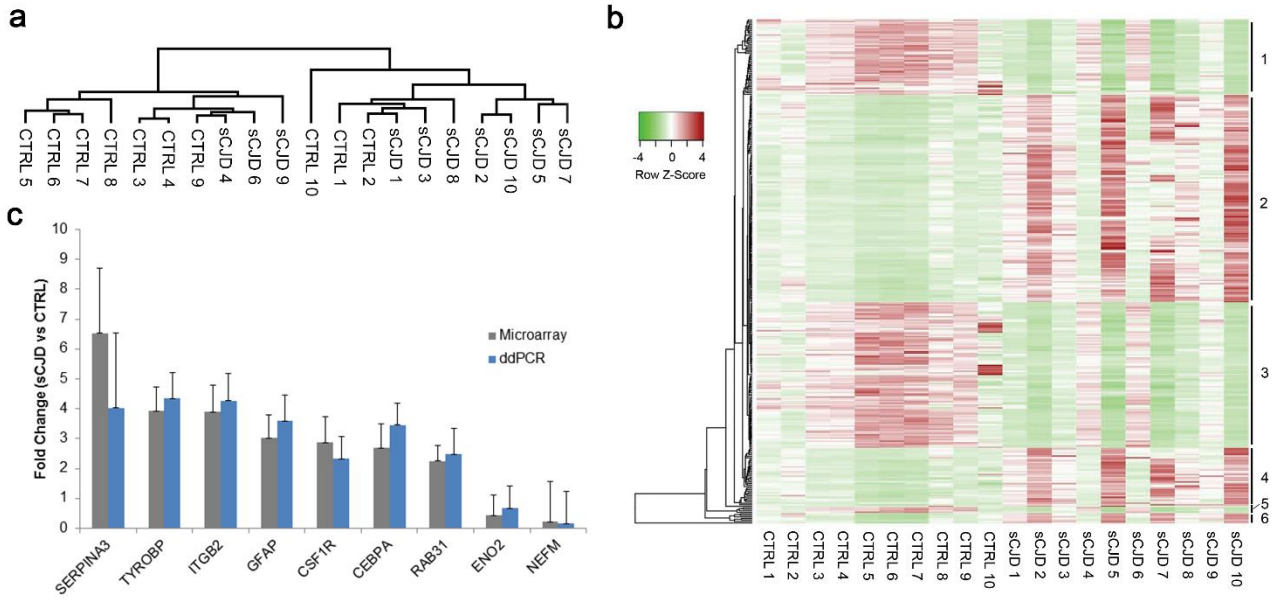
a
CTRL 5
CTRL 6
CTRL 7
CTRL 8
CTRL 3
CTRL 4
CTRL 9
sCJD 4
sCJD 6
sCJD 9
CTRL 10
CTRL 1
CTRL 2
sCJD 1
sCJD 3
sCJD 8
sCJD 2
sCJD 10
sCJD 5
sCJD 7
b
-4
0
4
Row Z-Score
1
2
3
4
5
6
CTRL 1
CTRL 2
CTRL 3
CTRL 4
CTRL 5
CTRL 6
CTRL 7
CTRL 8
CTRL 9
CTRL 10
sCJD 1
sCJD 2
sCJD 3
sCJD 4
sCJD 5
sCJD 6
sCJD 7
sCJD 8
sCJD 9
sCJD 10
c
Fold Change (sCJD vs CTRL)
Microarray
ddPCR
SERPINA3
TYROBP
ITGB2
GFAP
CSF1R
CEBPA
RAB31
ENO2
NEFM

Figure 1.

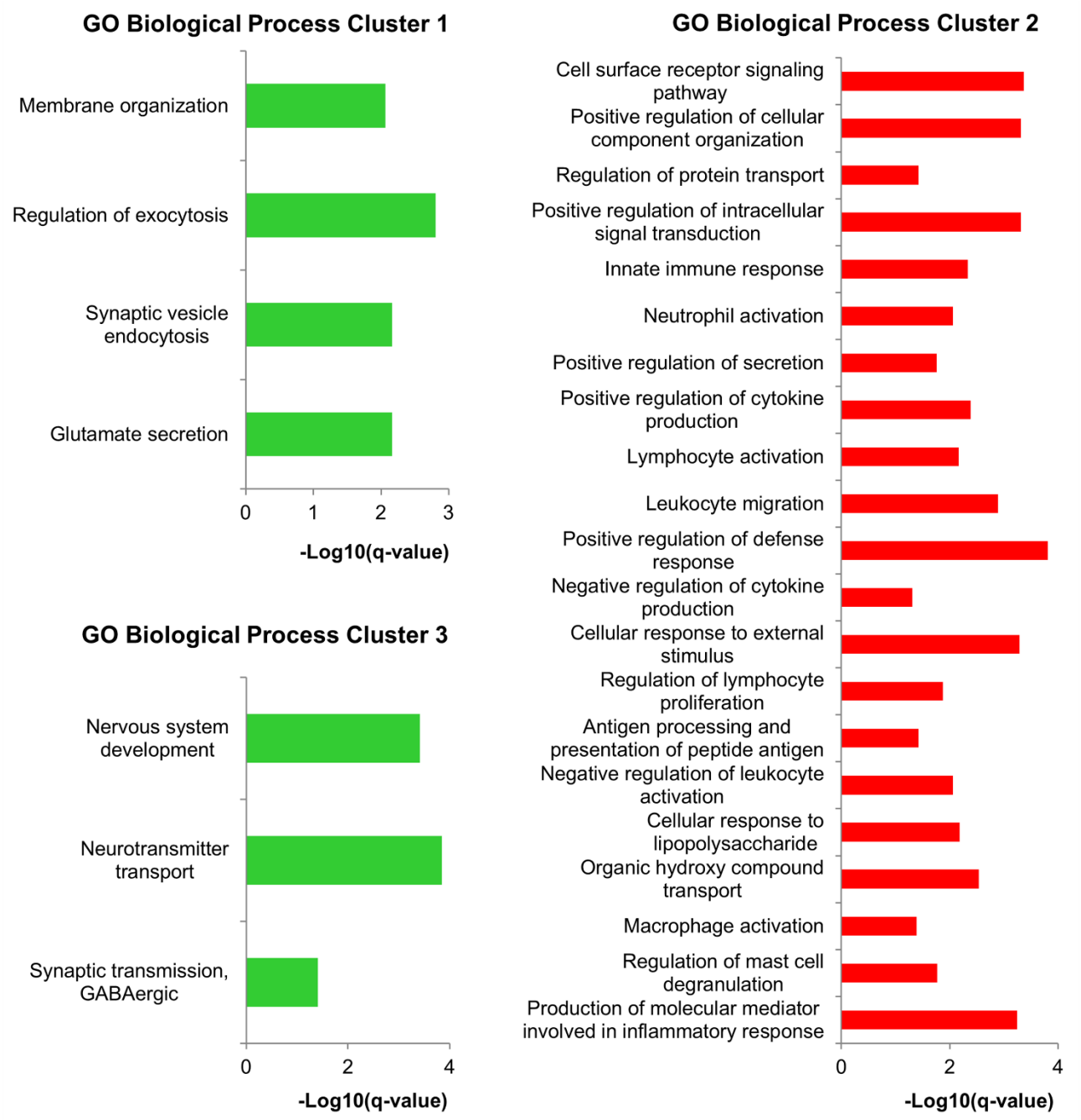
GO Biological Process Cluster 1
Membrane organization
Regulation of exocytosis
Synaptic vesicle endocytosis
Glutamate secretion
0
1
2
3
-Log10(q-value)
GO Biological Process Cluster 2
Cell surface receptor signaling pathway
Positive regulation of cellular component organization
Regulation of protein transport
Positive regulation of intracellular signal transduction
Innate immune response
Neutrophil activation
Positive regulation of secretion
Positive regulation of cytokine production
Lymphocyte activation
Leukocyte migration
Positive regulation of defense response
Negative regulation of cytokine production
Cellular response to external stimulus
Regulation of lymphocyte proliferation
Antigen processing and presentation of peptide antigen
Negative regulation of leukocyte activation
Cellular response to lipopolysaccharide
Organic hydroxy compound transport
Macrophage activation
Regulation of mast cell degranulation
Production of molecular mediator involved in inflammatory response
0
2
4
-Log10(q-value)
GO Biological Process Cluster 3
Nervous system development
Neurotransmitter transport
Synaptic transmission, GABAergic
0
2
4
-Log10(q-value)

Figure 2.

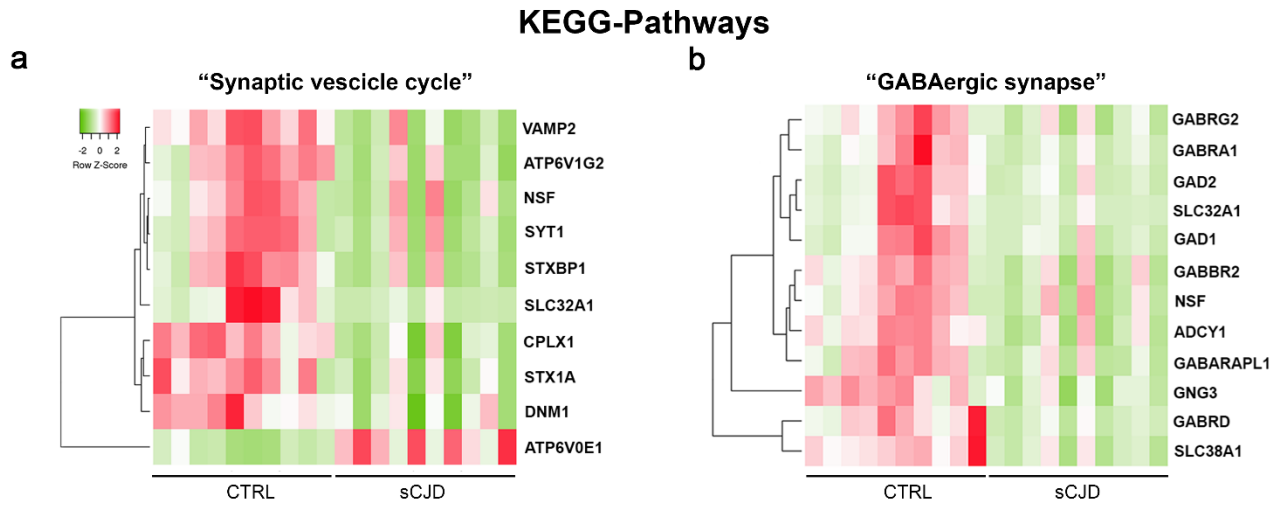
KEGG-Pathways
a
"Synaptic vescicle cycle"
-2 0 2
Row Z-Score
VAMP2
ATP6V1G2
NSF
SYT1
STXBP1
SLC32A1
CPLX1
STX1A
DNM1
ATP6V0E1
CTRL
sCJD
b
"GABAergic synapse"
GABRG2
GABRA1
GAD2
SLC32A1
GAD1
GABBR2
NSF
ADCY1
GABARAPL1
GNG3
GABRD
SLC38A1
CTRL
sCJD

Figure 3.

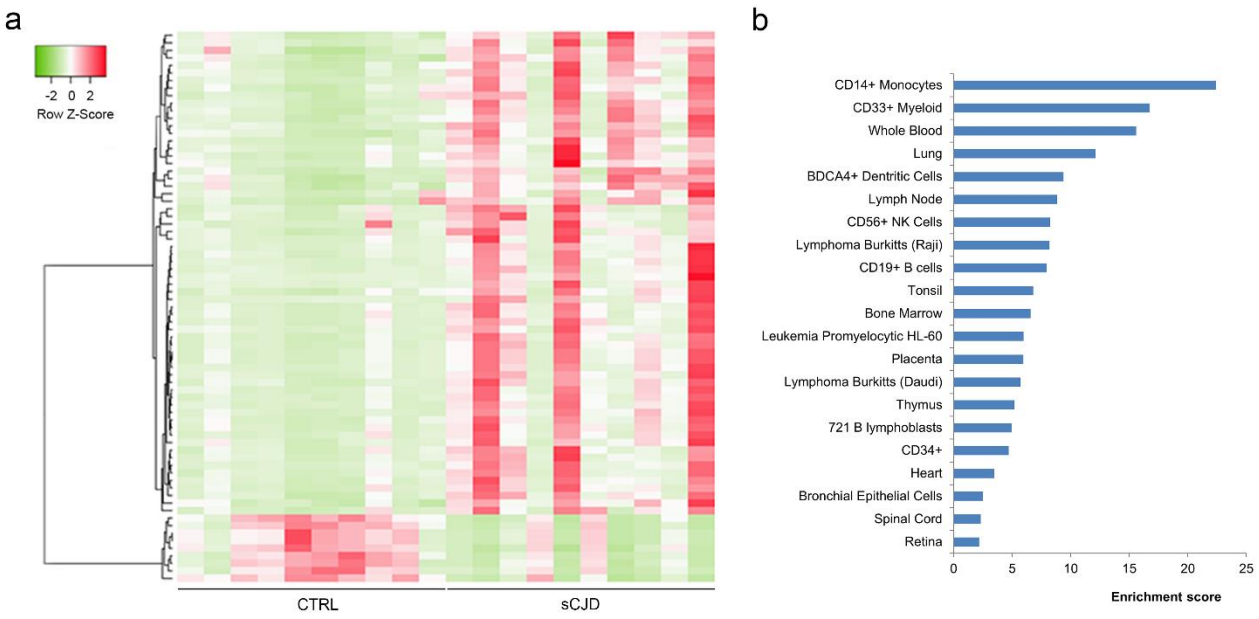
a
-2 0 2
Row Z-Score
CTRL
sCJD
b
CD14+ Monocytes
CD33+ Myeloid
Whole Blood
Lung
BDCA4+ Dentritic Cells
Lymph Node
CD56+ NK Cells
Lymphoma Burkitts (Raji)
CD19+ B cells
Tonsil
Bone Marrow
Leukemia Promyelocytic HL-60
Placenta
Lymphoma Burkitts (Daudi)
Thymus
721 B lymphoblasts
CD34+
Heart
Bronchial Epithelial Cells
Spinal Cord
Retina
0
5
10
15
20
25
Enrichment score

Figure 4.

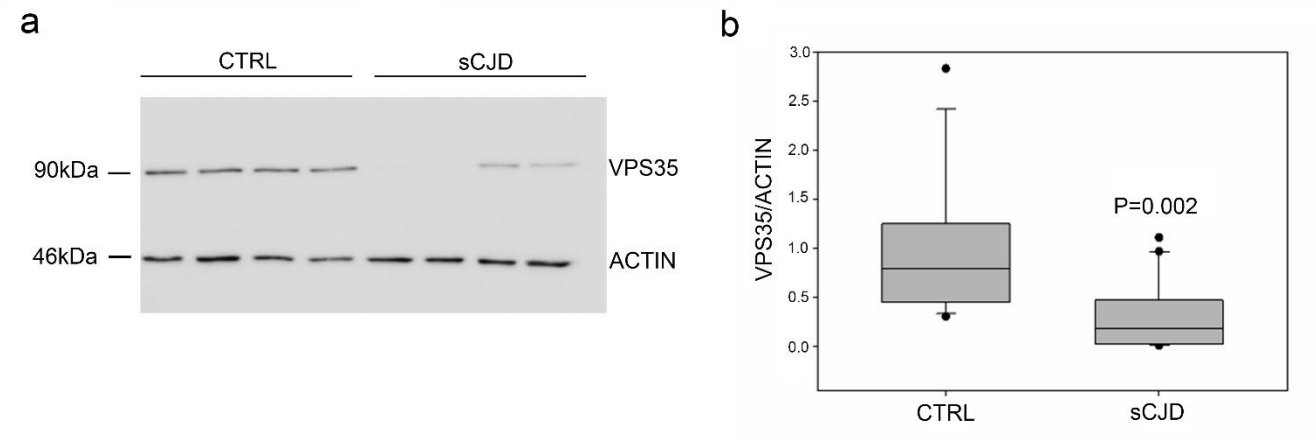
a
CTRL
sCJD
90kDa
46kDa
VPS35
ACTIN
b
VPS35/ACTIN
3.0
2.5
2.0
1.5
1.0
0.5
0.0
P=0.002
CTRL
sCJD

Figure 5.

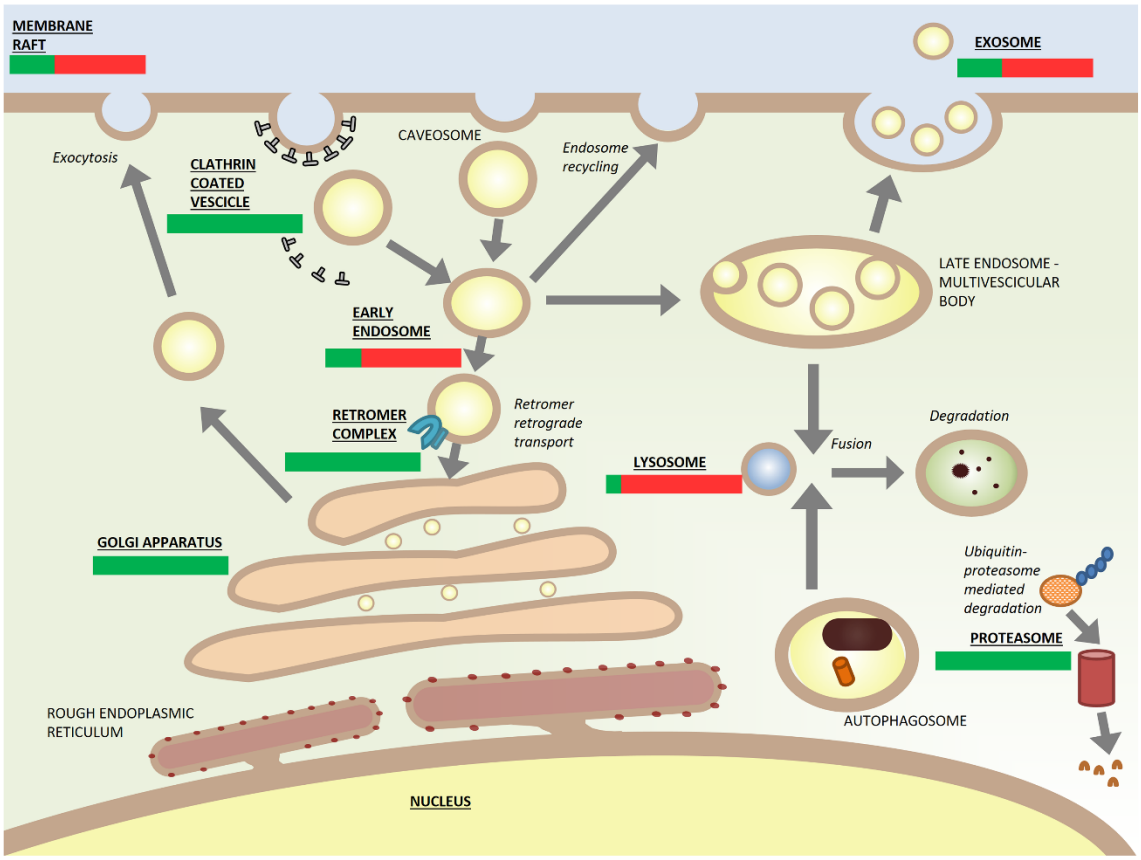

Membrane raft (Overrepresentation analysis - hDEGs) ↑ *HMOX1, RFTN2, LRP4, TNFRSF1A, RHOQ, LYN, BST2, SLC9A3R1, GJA1, ABCA1, SDC4, VIL2, OLR1, ITGB2* ↓ *MAL2, ADCY1, ATP1B1, ATP2B2, ATP1A1, RIT2*
Golgi Apparatus (Gene Set Enrichment Analysis – Genes core) ↓ *AP3B2, STEAP2, ICA1, AP1S1, DNM1L, DOPEY1, TRIM23, COG1, COPG, MAN1C1, OCRL, GNAS, LARGE, AFTPH, COPG2, NECAB3, ENTPD4, ARCN1, AP1G2, HS3ST1, RHOT2, KIAA0368, COPA, RAB11A, USO1, ATP2C1, SPG21, TGOLN2, TRAPPC4, COG6, B3GALT6, BET1, AP4B1, RHOT1, VPS45, TMED10, GGA3, GOPC, NBEA, ARFGEF2, COG5*
Lysosome (Overrepresentation analysis - hDEGs) ↑ *BGN, CD68, SLC11A1, NCAN, HLA-DPA1, NPC2, CTSH, TMBIM1, GPC5, LYN, SLC15A3, BST2, CD74, HLA-DMA, RNASET2, GJA1, VAMP8, SDC4, HLA-DMB, GFAP, HLA-DRA, LAPTM5, SERPINA3* ↓ *EPDR1, NSF, GOT1*
Extracellular Exosome (Overrepresentation analysis - hDEGs) ↑ *RAPGEF3, BBOX1, RENBP, PMP2, EFHD1, PLXDC2, BGN, RHOBTB3, P8, PSAT1, FKBP5, DOCK2, PTTG1IP, AEBP1, PLOD1, APOC2, ITGB5, BCAS1, NPC2, CTSH, TMBIM1, MSN, RHOQ, SLC2A5, LYN, APOE, BST2, CD74, SLC9A3R1, AKR1C3, HLA-DMA, RNASET2, GJA1, AXL, TSPO, ARHGDIB, VAMP8, VSIG4, ALDH1L1, SCIN, SDC4, VIL2, HLA-DRA, LCP1, SPP1, NQO1, OAF, FCGBP, OLR1, HAVCR2, ITGB2, HSPB1, C1QC, APOC1, C1QB, SERPINA3* ↓ *PVALB, STXBP1, UCHL1, BEX5, MAL2, ADCY1, CLSTN3, HPRT1, HPRT1, NAPB, CKMT1A, ATP1B1, ATP2B2, SPHKAP, ATP1A1, EPDR1, NSF, ENO2, TUBB3, MDH1, VAMP2, FGF9, FAM3C, BASP1, MAP4, DNM1, GOT1, SLC38A1*
Endosome (Overrepresentation analysis - hDEGs) ↑ *M6PRBP1, LY96, NTRK2, CD68, APOC2, SLC11A1, HLA-DPA1, ATP6V0E1, RAB31, CTSH, TMBIM1, APOE, BST2, CD74, HLA-DMA, GJA1, SYTL4, VAMP8, CYBA, HLA-DMB, VIL2, HLA-DRA, HAVCR2* ↓ *DYNC1I1, STMN2, PAK1, EPHA4, ATP1A1, NMNAT2, PACSIN1, PTPRN, SCAMP5*
Clathrin coated vesicle (Gene Set Enrichment Analysis – Genes core) ↓ *RAB3A, AP1G2, AFTPH, SLC30A3, AP1S1, DMXL2, STEAP2, ICA1, AMPH, SVOP*
Proteasome complex (Gene Set Enrichment Analysis – Genes core) ↓ *PSMC5, SHFM1, PSMD12, PSMC2, PSMD8, PSMD4, PSMD10, PSMD14, KIAA0368, PSMD7, PSMD3, PSMD1, PSMC4*
Retromer complex (Protein expression) ↓ VPS35

Figure 6.